



## Biomechanical wall properties of human intracranial aneurysms resected following surgical clipping

Vincent Costalat, Mathieu Sanchez, Dominique Ambard, L. Thines, Nicolas Lonjon, Franck Nicoud, H. Brunel, J.P. Lejeune, Henri Dufour, P. Bouillot, et al.

### ► To cite this version:

Vincent Costalat, Mathieu Sanchez, Dominique Ambard, L. Thines, Nicolas Lonjon, et al.. Biomechanical wall properties of human intracranial aneurysms resected following surgical clipping. Journal of Biomechanics, 2011, 44 (15), pp.2685-2691. 10.1016/j.jbiomech.2011.07.026 . hal-00686616

**HAL Id: hal-00686616**

**<https://hal.science/hal-00686616>**

Submitted on 24 Apr 2012

**HAL** is a multi-disciplinary open access archive for the deposit and dissemination of scientific research documents, whether they are published or not. The documents may come from teaching and research institutions in France or abroad, or from public or private research centers.

L'archive ouverte pluridisciplinaire **HAL**, est destinée au dépôt et à la diffusion de documents scientifiques de niveau recherche, publiés ou non, émanant des établissements d'enseignement et de recherche français ou étrangers, des laboratoires publics ou privés.

1 Biomechanical wall properties of human intracranial  
2 aneurysms resected following surgical clipping  
3 (IRRA Project\*)  
4  
5

6 V. Costalat, M. Sanchez, D. Ambard, L. Thines, N. Lonjon, F. Nicoud, H. Brunel, J.P. Leje-  
7 une, H. Dufour, P. Bouillot, JP Lhaldky, K. Kouri, F. Segnarbieux, CA Maurage, K. Lobote-  
8 sis, M.C. Villa-Uriol, C. Zhang, A.F. Frangi, G. Mercier, A. Bonafé, L. Sarry, and F. Jourdan.

9  
10 \* The research consortium “Individual Risk Rupture Assessment of Intracranial aneurysm”  
11 (IRRA) was founded by 4 clinical centers, and 3 European laboratories in France, and Spain.  
12  
13

14 **Classification = Original Research**  
15

16 **Word count:** Main Text and Abstract = 2829  
17  
18

19 BM-D-11-00205  
20  
21

22 **Contact information:**

23 Vincent Costalat, MD, PhD ([vincentcost@hotmail.com](mailto:vincentcost@hotmail.com))

24 CHU Montpellier, Interventional Neuroradiology, Av Augstin Fliche, Montpellier, France.  
25  
26  
27

27

28

29 **All authors have made substantial contributions to all of the following:**

30 (1) the conception and design of the study; VC;DA;FJ;FN;MS

31 (2) acquisition of data; VC;MS; LT;NL;JPL;FS;HD;HB;PB;JPH;CAM;KK;AB

32 (3) analysis and interpretation of data; GM;VC;FJ;DA;MS

33 (4) drafting the article or revising it critically for important intellectual content;

34 VC;MS;FJ;KL;DA;FN;LS;AFF

35

35

36

37

38

38

39 **Abstract:**

40 **Background and Purpose**— Individual rupture risk assessment of intracranial aneurysms is a  
41 major issue in the clinical management of asymptomatic aneurysms. Aneurysm rupture occurs  
42 when wall tension exceeds the strength limit of the wall tissue. At present, aneurysmal wall  
43 mechanics are poorly understood and thus, risk-assessment involving mechanical properties is  
44 inexistent. Additionally, aneurysmal computational hemodynamics usually makes the as-  
45 sumption of rigid walls, an arguable simplification. We therefore aim to assess mechanical  
46 properties of ruptured and unruptured intracranial aneurysms in order to provide the founda-  
47 tion for future patient-specific aneurysmal risk assessment. This work will also challenge  
48 some of the currently held hypotheses in computational flow hemodynamics research.

49 **Methods**—A specific conservation protocol was applied to aneurysmal tissues following clip-  
50 ping and resection in order to preserve their mechanical properties. **Sixteen intracranial** an-  
51 eurysms (11 female, 5 male) underwent mechanical uni-axial stress tests under physiological  
52 conditions, temperature, and saline isotonic solution. These represented 11 unruptured and 5  
53 ruptured aneurysms. Stress/strain curves were then obtained for each sample, and a fitting  
54 algorithm was applied following a 3-parameter ( $C^{10}$ ,  $C^{01}$ ,  $C^{11}$ ) Mooney-Rivlin hyperelastic  
55 model. Each aneurysm was classified according to its biomechanical properties and  
56 (un)rupture status.

57 **Results**— Tissue testing demonstrated three main tissue classes: Soft, Rigid, and Intermedi-  
58 ate. All unruptured aneurysms presented a more Rigid tissue than ruptured or pre-ruptured  
59 aneurysms within each gender subgroup. Wall thickness was not correlated to aneurysmal  
60 status (ruptured/unruptured). An Intermediate subgroup of unruptured aneurysms with softer  
61 tissue characteristic was identified and correlated with multiple documented risk factors of  
62 rupture.

63 **Conclusion:** **A significant biomechanical properties modification between ruptured an-**  
64 **eurysm, presenting a soft tissue and unruptured aneurysms, presenting a rigid material**  
65 **was observed. This finding strongly supports the idea that a biomechanical-based risk**  
66 **factor can and should be developed in the near future to improve the therapeutic deci-**  
67 **sion making.**

68

68

69

70 **Introduction:**

71 The prevalence of unruptured intracranial aneurysms in the general population, as reported by  
72 a recent review,<sup>1</sup> ranges between 3% and 6.6%. The incidence of ruptured aneurysms is how-  
73 ever, low, with approximately 0.5% per year suggesting that very few aneurysms rupture.  
74 Subarachnoid hemorrhage is the consequence of aneurysm rupture and approximately 12% of  
75 patients die before receiving medical attention, 40% of hospitalized patients die within one  
76 month after the event, and more than one third of those who survive have major neurological  
77 deficits. In contrast endovascular treatment of unruptured aneurysms is safe with less than 1%  
78 mortality rate<sup>2</sup>. Unruptured intracranial aneurysms represent a dilemma for the physicians.  
79 The risks of aneurysm rupture with respect to its natural history against the risk of morbidity  
80 and mortality from an endovascular or surgical repair has to be carefully balanced. With brain  
81 imaging being more frequently and widely used, a growing number of intracranial aneurysms  
82 are being diagnosed, posing the problem of which aneurysms harbor a sufficiently high risk of  
83 rupture to merit endovascular or surgical repair. Recent publications have addressed this issue  
84 and have demonstrated that, among other variables affecting the natural history of aneurysms,  
85 aneurysm size and location represent independent predictors of rupture risk<sup>3</sup>. Other param-  
86 eters, such as irregular aneurysm shape and, in particular, the presence of blebs<sup>4, 5</sup> are recog-  
87 nized as high risk factors.

88 Rupture of an aneurysm occurs when wall tension exceeds the strength limit of the wall tis-  
89 sue. The ideal approach to risk assessment would therefore be to determine tension and mate-  
90 rial strength limits of the tissue<sup>6</sup> in the aneurysmal wall. Individual aneurysmal material  
91 strength is impossible to measure non-invasively, but wall tension can be estimated using  
92 computational simulation<sup>7</sup>. Over the last decade, a number of authors have shown that com-  
93 putational fluid dynamic simulations based on patient-specific anatomical models derived  
94 from medical imagery may be used to assess wall shear stress (WSS) and pressure in the Cir-  
95 cle of Willis<sup>8, 9, 10</sup>. Others have used the same approach to analyze cerebral aneurysms, with  
96 particular focus on WSS, which is thought to be associated with aneurysm formation and risk  
97 rupture.<sup>11, 12, 13</sup> Although simulation of aneurysmal wall tension is now feasible in principle,  
98 real human aneurysmal wall biomechanical properties are still rarely explored in the litera-  
99 ture.<sup>14, 15</sup> Computational simulations must be based on reliable material properties and

boundaries. As opposed to hemodynamic boundary conditions that may be assessed by Phase Contrast-MRI or transcranial Doppler, in vivo, patient specific measurements of tissue properties are not feasible yet. Most of the current research on computational hemodynamics assumes uniform wall thickness and wall properties based on average values extracted from the scarce available literature. Although some of these assumptions may be acceptable in practice, no in-depth study has demonstrated their validity thus casting shadows on the accuracy of the current computational hemodynamics work. For this purpose a research consortium (**IRRA**s for **I**ndividual **R**isk **R**upture **A**ssessment of Intracranial Aneurysm) was founded between 3 research Laboratories and 4 French neurosurgical centers (Montpellier, Lille, Nimes and Marseille) and involving corresponding departments of neuroradiology and anatomopathology. The first purpose of the **IRRA**s consortium is to build a database of aneurysmal biomechanical parameters. Such database will be instrumental in supporting new computational strategies to determine the risk of rupture in cerebral aneurysms based on patient-specific imaging data and domain-specific biomechanical knowledge.

**The purpose of this study is to explore the biomechanical behavior characteristics of ruptured and unruptured aneurysms. Building such database is a mandatory to establish the idea that the rheology of the tissue correlates with the status of the aneurysm and that a biomechanical-based risk rupture factor can indeed be developed.**

118

## 119 **Materials and methods**

### 120 ***Surgical technique and aneurysm selection***

121 Eighteen patients treated for ruptured or unruptured aneurysms by surgical clipping were re-  
122 cruited by 4 French neurosurgical teams. The research study protocol was approved by the  
123 local ethical committee in each center. A consent form was signed by patients with normal  
124 neurological status, or by the relatives in all other cases. Following surgical clipping (Fig.1)  
125 angio fluoroscopy imaging was performed by the neurosurgeon to control aneurysm sac ex-  
126 clusion. Once the distal aneurysm was confirmed to be safely excluded from the circulation,  
127 the neurosurgeons removed it in one piece. In this way, 18 intact aneurysms samples were  
128 then extracted from 17 patients.

### 129 ***Clinical and Radiological Data***

130 **For each patient, clinical, and radiological information was collected concerning age,**  
131 **gender, aneurysm status (ruptured/unruptured), size (measured from the dome of the**  
132 **aneurysm and the neck represented by the communication of the aneurysm with the**  
133 **parent artery), the “dome to neck” ratio (aneurysm size/neck length), location on the**  
134 **Willis circle, morphological evaluation (classified "simple shaped" for regular unilobu-**  
135 **lated aneurysm and "complex shaped" for multilobulated and irregular aneurysm), as**  
136 **well as documented rupture risk factors; multiple aneurysms, previous ruptured aneu-**  
137 **rysm, positive family history of ruptured intracranial aneurysm, autosomal dominant**  
138 **polycystic kidney disease, hypertension, alcohol and tobacco.** A possible mycotic intracra-  
139 nial aneurysm etiology was considered an exclusion criterion, as well as any previous history  
140 of endocarditis and inflammatory disease. **All documented risk factors were then recorded**  
141 **in order to be related to the biomechanical behavior of each aneurysm.**

### 142 ***Aneurysm Sample Conservation protocol***

143 In order to conserve the mechanical properties of the aneurysm wall, a specific conservation  
144 protocol was applied in each center by means of a dedicated histopathological removal kit  
145 available in the neurosurgical operating room. The resected aneurysm was initially inserted in  
146 a tube containing a Ringer lactate, 10% DMSO solution. This first tube was then placed in a  
147 larger second one containing isopropanol. This combination of the two tubes was placed in a  
148 freezer (-80°C). The sample was progressively frozen due to the surrounding isopropanol so-  
149 lution in order to maintain its biomechanical properties<sup>16</sup>. Frozen samples were then stored in



the anatomopathology department of the neurosurgical center, before mechanical testing was carried out.

### ***Biomechanical testing methodology***

One hour before mechanical testing, aneurysms sample were thawed at ambient temperature. Under microscopy, the aneurysmal wall samples were dissected in a meridional manner in order to obtain a regular rectangular piece (Fig.2). **Only the meridional axis of the aneurysm was chosen in order to preserve maximum length of the aneurysmal tissue in the sample given the very small size of each specimen and the fragility of the tissue.** The aneurysm strips were physically measured and then glued on each extremity to aluminum grips. Meanwhile, physiological isotonic liquid was warmed to 40°C inside the traction test machine. A uniaxial stretch test was carried out on the sample within the warmed physiological liquid in order to simulate the in vivo conditions (Fig. 3a). This testing device was composed of a Texture Analyzer (TA-XT2, Stable Microsystems, UK) with a 50 N load cell and an optical microscope (ZEISS) equipped with a digital video camera .

The uniaxial stretch test consisted of a sequence of 10% length displacement of the sample, in 5 repeated cycles (Fig. 3b), while registering the traction force applied. This 10% value was initially calculated by Karmonik et al.<sup>17</sup> in an in-vivo wall motion MRI study of 7 aneurysms. **In accordance to standard mechanical testing protocol for biological tissue, the specimens were first preconditioned<sup>18</sup> during the first four cycles.** The extension rate was 0.01 mm/s and the tension load was recorded every 0.01 s. Velocity of the solicitations was small enough to not consider viscous phenomena. A baseline tension of 0 Newton was applied to the strip before starting each test, and two cameras were orthogonally placed and focused on the sample after a calibration test

During the test, the two subset cameras were used to record the displacement of the sample. These images were subsequently used to determine the exact **dimensions** of the strips (resolution of 4µm/pixel). A Force/Displacement graph was obtained **from each sample testing allowing tissue characterization**

## Post processing

Only the measurements from the last elongation cycle were used in order to obtain more realistic mechanical characterization of the data. Note however that except for the very first cycle, the force/displacement graph was roughly cycle independent (fig 3 b).. In order to tune the parameters of an equivalent hyperelastic model, the force/displacement graph described above was converted in a strain/stress graph. For this calculation, the length, thickness and width of each strip were considered (Fig. 3b). A baseline for this aneurysmal **strip dimensions** were obtained at 0-Newton traction in the third cycle of each test. Using the assumption that the specimen was subjected to a uniform traction and presented a constant section during the test, the Cauchy stress was computed, and the engineering strain registered<sup>19, 20</sup>.

During the cycles some permanent deformation in the traction phase was observed causing slight compression of the sample in the rest phase. This is reflected by the negative values of the curve origin in Figure 3b and is in accordance to the elasto-plastic behavior of the tissue. Since we consider an hyperelastic model to represent the tissue, the (moderate) plastic effects cannot be represented and only the positive part of the curve was used to identify material behavior.

Once the strain/stress graph was obtained, we proceed to a mathematical matching using a Sequential Least Squares Programming algorithm in order to determine the corresponding hyperelastic model and its coefficients. In our cases, the best match was obtained with a 3 parameters Mooney-Rivlin model<sup>21, 22</sup>. Let  $F$  be the measured load,  $S_0$  the initial section and  $\lambda$  the elongation of the sample, the behavior law is given by equation (1)..

$$(1) \frac{F}{S_0} = 2(\lambda - \lambda^{-2}) \left( c_{10} + c_{01} \lambda^{-1} + c_{11} (3\lambda^{-2} + 3\lambda - 3 - 3\lambda^{-1}) \right)$$

where the material parameters are  $C_{10}$ ,  $C_{01}$  and  $C_{11}$ . The values of each of these coefficients for each aneurysm are gathered in Table 1 together with **strip dimensions** and relevant clinical factors.

## Statistical analysis

The aneurysmal wall characteristics were presented using median and range for continuous variables and frequencies and proportions for categorical variables. Groups (defined by biomechanical status and material property) were compared using non-parametric Wilcoxon

rank test for continuous variables and Fisher exact test for categorical ones. Statistical significance threshold was set at 5%. Statistical analyses were performed using SAS version 9.1 (SAS Institute, Cary, North Carolina).

## **Results:**

### ***Population:***

Eleven unruptured and five ruptured aneurysms were included in the study. In one unruptured aneurysm case, pre-rupture symptoms with acute headache, and recent vision loss secondary to optic nerve compression was reported and highlighted in the table 1. Mean age was 46.7 (min 32 – max 64). Location was middle cerebral artery (MCA) in 9 cases (56.6%), anterior communicating artery (AComA) in 3 cases (18.7%), posterior communicating artery (PComA) in 2 cases (12.5%), and internal carotid artery (ICA) in 2 cases (6%). Aneurysm size is ranging from 4.2 to 13 mm.

### ***Sample and Mechanical testing:***

Out of the 16 surgically clipped aneurysms that were subjected to mechanical uniaxial strain tests, 11 were from female and 5 from male patients (Sex Ratio = 0.45). Mean strip length was 4.8 mm (ranging from 1.3 to 8), with a mean thickness of 370  $\mu\text{m}$  (ranging from 170 to 680  $\mu\text{m}$ ), and a mean section surface of 0.62  $\text{mm}^2$  (ranging from 0.29 to 1.6  $\text{mm}^2$ ).

The coefficient  $C_{10}$  value ranged from 0 to 0.9 Mpa with a mean value of 0.19 Mpa,  $C_{01}$  ranged from 0 to 0.13 Mpa with a mean value of 0.024,  $C_{11}$  ranged from 0.124 to 32 Mpa with a mean value of 7.87.

To facilitate analysis, aneurysms were classified according to their status Ruptured/Unruptured and their biomechanical behavior Rigid/Soft/Intermediate (see Tables 1 and 2).

***Comparison of biomechanical parameters value among ruptured and unruptured aneurysms are summarized in tables 3, 4, and 5.***

## **Discussion**

### ***Results analysis***

A recent case-control study<sup>23</sup> on 4000 patients based on genetic variation suggests that the underlying mechanism for intracranial aneurysm pathogenesis may differ between male and female subjects, underlining the importance of a stratified analysis between genders. A significant difference in biomechanical parameters between ruptured and unruptured aneurysms was observed in our data within each gender group (Tables 3, 4, 5), therefore supporting the above statement.

Interestingly, the  $C_{11}$  coefficient, which represents the main curvature of each graph was the most representative parameter of this observed biomechanical difference (Table 3,  $p < 0.004$ ). The first two coefficients  $C_{01}$ ,  $C_{10}$  presented a low value (near 0) and were not significantly different ( $p = 0.4$  and  $p = 0.7$ ) regarding aneurysmal status (ruptured/unruptured). All  $C_{11}$  values were observed below 1.2 MPa (mean 0.37 MPa) in ruptured or pre ruptured female aneurysms, and below 3.2 MPa (mean 3.1 MPa) in male ruptured aneurysms.

In the female group, all the unruptured aneurysms presented a more rigid behavior than the ruptured or pre-ruptured aneurysms ( $C_{11} = 0.48$  vs 11.7 MPa;  $p < 0.001$ , Table 4). Between the unruptured aneurysms, we can distinguish two subgroups; the Unruptured/Rigid patients (#2-#7-#9) and the Unruptured/Intermediate patients (#8-#10-#11-#15). In this last subgroup representing an unruptured aneurysm with a softer aneurysmal wall, three out of four presented either documented major epidemiologic risk factors or a radiologically high risk shape (multilobulated). Only one aneurysm (#15) was simple shaped without further associated risk factors in this subgroup. One single patient (#16) presenting an unruptured aneurysm was classified as Soft with similar material properties with the Ruptured group. In this particular case, pre-rupture symptoms with major headache, and recent optic nerve compression were recorded few days before surgery and motivated urgent treatment. Therefore, in this case, the mechanical test findings of Soft may not be as paradoxical as thought of at the first glance.

In the male group, all the unruptured aneurysms tended have Rigid material than the ruptured ones ( $C_{11} = 11.95$  vs 3.17 MPa;  $p = 0.058$ , Table 5). Similarly to the female, unruptured aneurysms can be split in two subgroups, with 2 aneurysms classified Unruptured/Intermediate (Aneurysm #12 and #14), and one aneurysm classified Unruptured/Rigid. Among the Intermediate/Unruptured aneurysms one presented a major documented risk factor with multiple aneurysms, in accordance to a possible underlying connective tissue disease. Interestingly, in the male group, the ruptured aneurysms (Aneurysms #5 and #13) had a thicker wall compared to the Intermediate/Unruptured aneurysms, in contradiction to common conceptions, and in accordance to previous histopathologic work<sup>24</sup>.

Rheological data relevant to aneurysmal tissue are very scarce in the literature. To the authors' knowledge, the only previous study is by Toth et al.<sup>22</sup> who also gained insights about the tissue rheology from 1D traction testing. Unfortunately, no subgroup analysis among ruptured or unruptured status was performed by Toth et al. and the significant parameter  $C_{11}$  was not calculated. Still, the initial mean tangent modulus they obtained for their hyperelastic model can be compared to the  $C_{01}+C_{10}$  parameter from the previous study. For the women group, this initial tangent modulus was evaluated from  $2.79 \cdot 10^{-2}$  to  $22.4 \cdot 10^{-2}$  Mpa vs whereas it is in the range  $1.905 \cdot 10^{-2}$  to  $77.05 \cdot 10^{-2}$  in our study. For the men group, this value was measured from  $2 \cdot 10^{-2}$  to  $25.3 \cdot 10^{-2}$  Mpa vs from  $10.15 \cdot 10^{-2}$  to  $93.74 \cdot 10^{-2}$  in our study. From the results presented in this study, reproducible material characteristics were observed among the ruptured and pre-ruptured aneurysms with similar biomechanical behavior, suggesting a same vulnerable status of the aneurysmal wall in a rupture or pre-rupture status. These two behaviors were significantly different from the unruptured aneurysms, presenting a rigid tissue. At the same time, there was no statistical correlation observed between the thickness of the wall, the aneurysm size and the Ruptured/Unruptured aneurysms status. This observation supports the hypothesis that the aneurysm wall vulnerability is directly related to the tissue microstructure<sup>25</sup>, and not to a progressive wearing of the wall.

The evolution of aneurysmal biomechanical properties was modeled by Watton et al. et al.<sup>26</sup> who performed numerical simulations of aneurysmal initiation and growth and postulated a degradation model of the elastin layer. Furthermore, a previous histopathology study<sup>25</sup> demonstrated that prior to rupture, the wall of cerebral aneurysm undergoes morphological changes associated with degeneration and repair.

**The main contribution of our study has been to demonstrate a very significant biomechanical property difference between pre-rupture or rupture aneurysms with a soft tissue and unruptured aneurysm with a Rigid tissue (Fig.6).**

### *Limitation of the study*

Because of the surgical resection necessary to obtain these samples, only aneurysms easily and safely accessible were selected, introducing a potential selection bias in this study. Hence, the MCA location was over-represented. There may be also a bias induced by the differences between cases with indication of surgical treatment compared to those indicated for interventional therapy. Nevertheless we observed aneurysm size ranging from 4.2 to 13 mm representing the majority of aneurysms treated to date. Within the statistical limitations of our sample, we could not observe any significant difference in mechanical properties of the aneurysmal wall according to the location. Interestingly, in the patient harboring two aneurysms (aneurysm #10 and #11) in different locations (ICA and MCA, respectively), we observed similar mechanical properties.

Uniaxial strain/stress testing is not representative of the anisotropic behavior of the aneurysm wall in vivo. **Although, bi-axial testing was contemplated in this study, it is technically challenging to carry out. In our experiments the main limitation was the small size of the strips ranging from 1.2 to 8 mm. Work by Toth et al.<sup>15</sup> also confirms that bi-axial testing does not generate reliable and reproducible results.** MacDonald et al.<sup>30</sup> investigated the molecular strength of the collagen fibers layers in 4 aneurysms. When comparing directional tissue strength, an anisotropy was demonstrated by a factor of 2. **In our study, aneurysm samples were selected in a meridional direction in both groups demonstrating a difference between ruptured and unruptured aneurysm in this direction. A bi-axial testing of the sample would have been a response to this high level of anisotropy, but these tests were not possible in our experience due to the very small size of the aneurysms.**

Furthermore, the probability of consistently and systematically slicing the aneurysm sample in the weakest direction in the ruptured aneurysms, and the strongest direction in unruptured aneurysms was unfeasible.

### **Conclusion**

Gender stratification was necessary to interpret the biomechanical testing. Within each gender subgroup; ruptured aneurysms presented lower Rigidity than ruptured aneurysms, supporting the hypothesis that there is a change in the biomechanical properties of the aneurysm wall

preceding rupture. Secondly, wall thickness was not correlated to ruptured/unruptured status. An Intermediate subgroup of unruptured aneurysms characterized by material properties corresponding to softer tissue was identified, and associated with multiple well documented risk factors of aneurysm rupture. Further studies about the biomechanical properties of cerebral aneurysms can help elucidating the biomechanical conditions preceding rupture. With the recent progress in *in vivo* aneurysm wall motion estimation<sup>17,31</sup> it may be possible soon to estimate *in vivo* mechanical material properties of cerebral aneurysms<sup>32,33</sup>. Such biomechanical parameters might be themselves good predictors of aneurysm rupture or might be integrated within a more comprehensive pipeline for image-based patient-specific simulations of fluid-wall structure interaction that renders a personalized estimate of the presence of vulnerable aneurysmal wall tissue and a potential increased rupture risk.

345  
346  
347

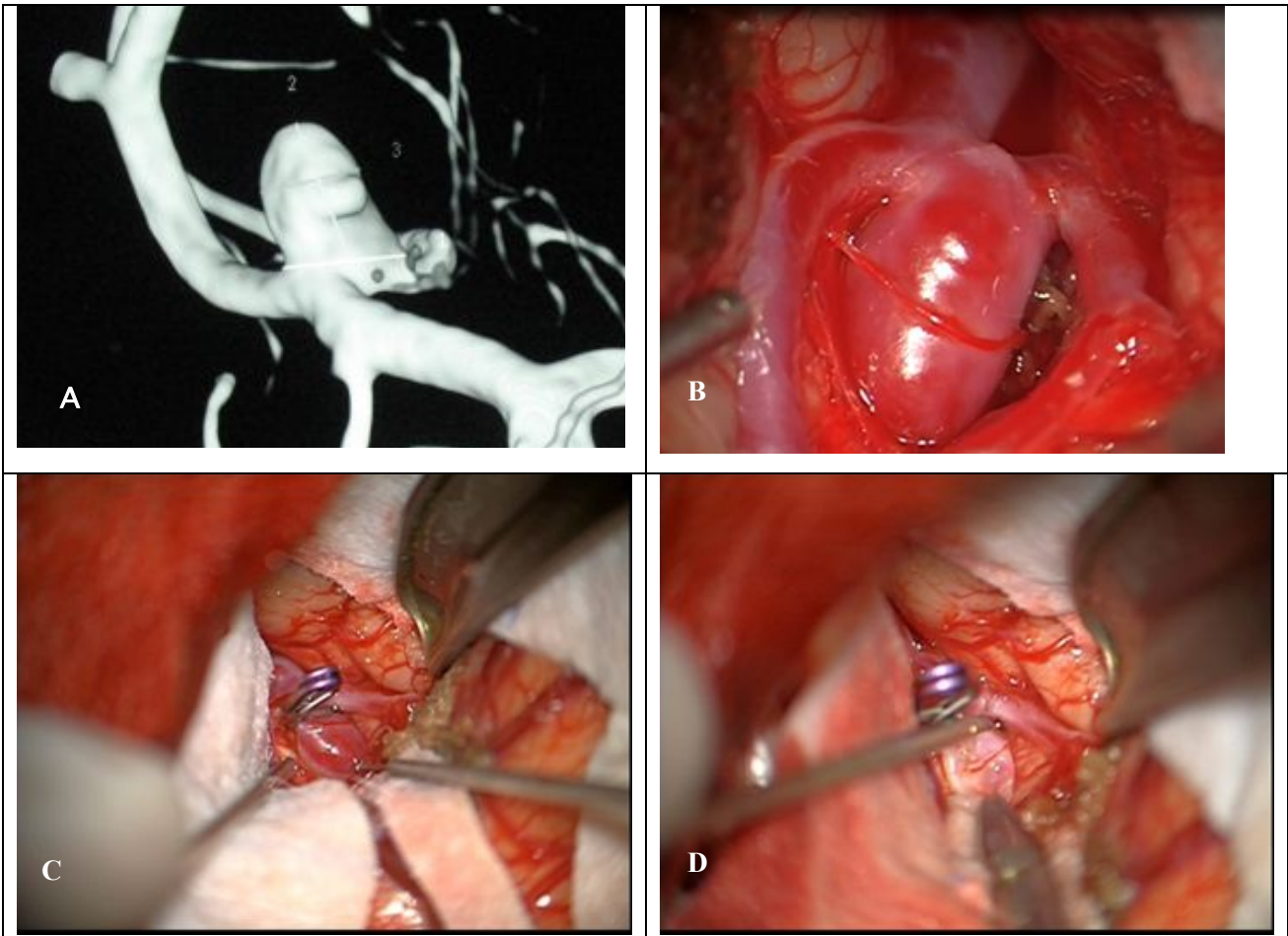
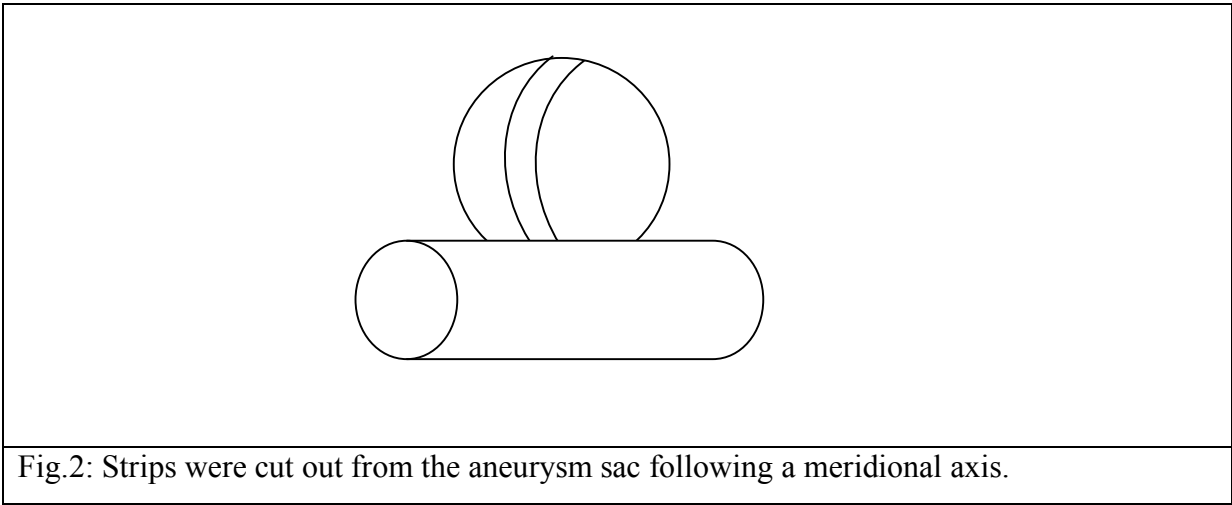


Fig. 1. (A) Three-dimensional rotational angiography imaging from Aneurysm #9. (B) Surgical view of this aneurysm in Middle Cerebral Artery location before clipping. (C)Aneurysm sac after surgical clipping. (D) Aneurysm resection.

348  
349



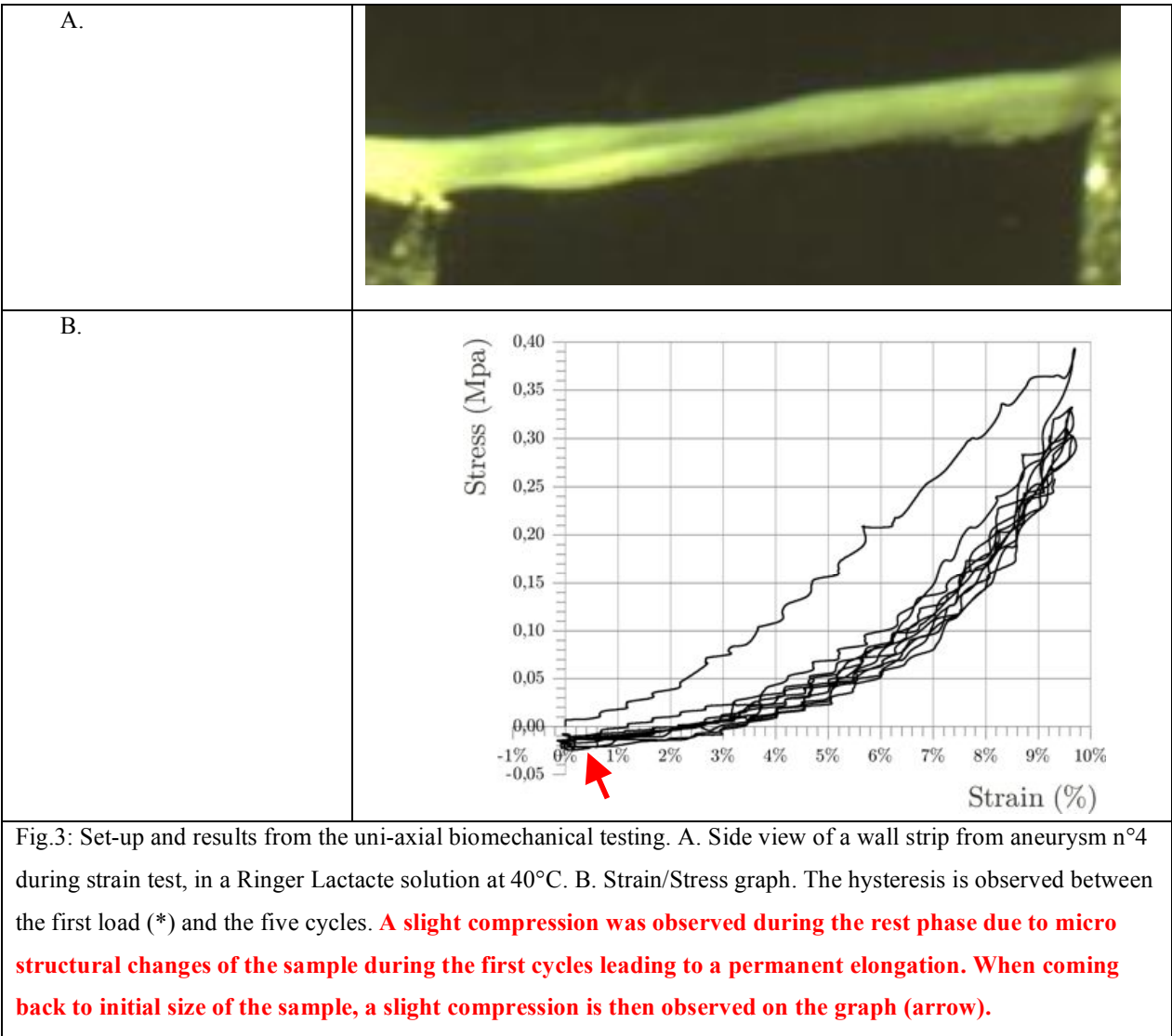
349



350

351

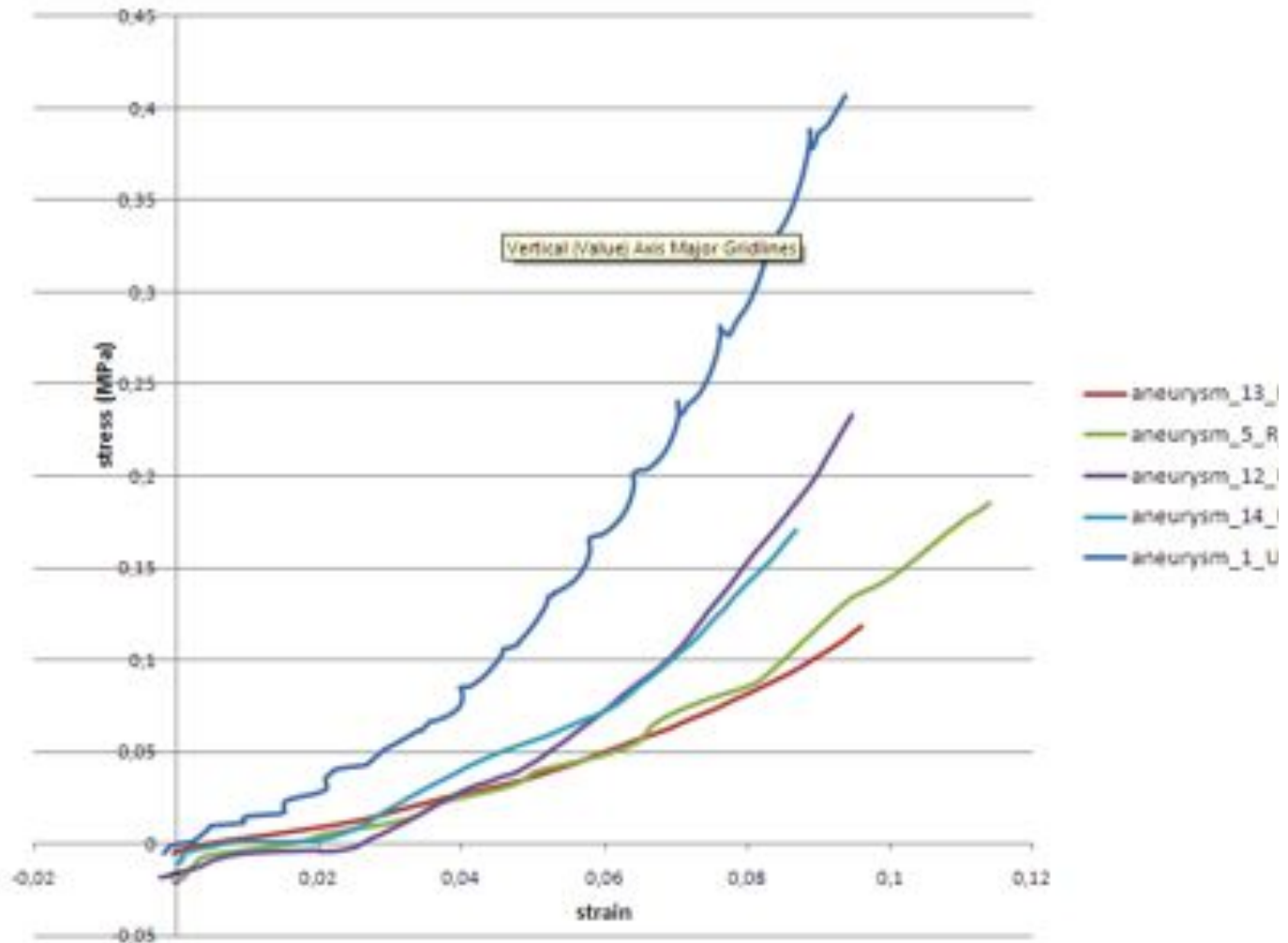
351

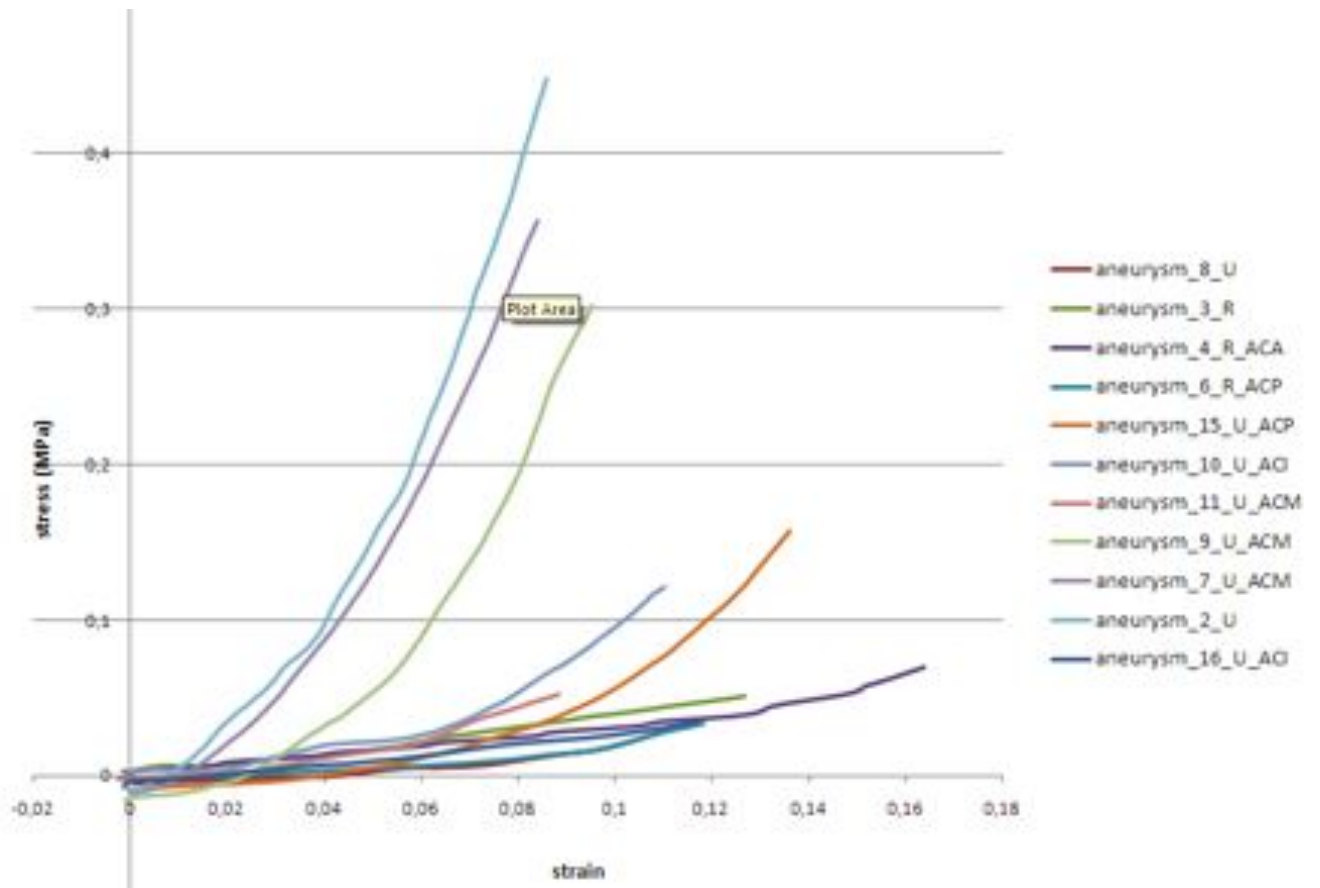


352

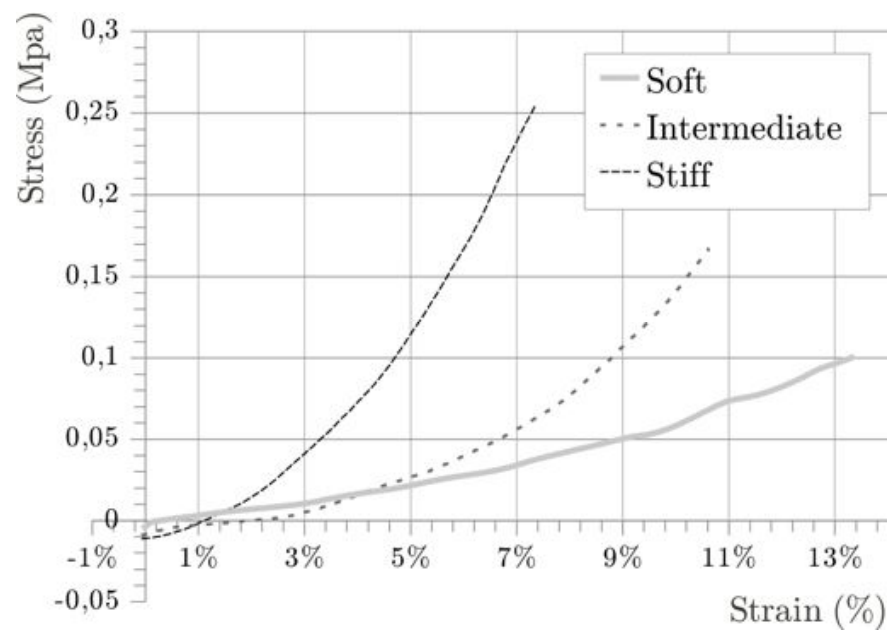
353

Fig. 4: Plots of the strain/stress relationships measured for men (R=ruptured, U=unruptured, ACA = Anterior Cerebral Artery, ACM=Middle Cerebral Artery)





378  
379



380  
381 Fig.6: Mean strain/stress curves representing the biomechanical tissue classification.  
382  
383

**Table 1:** Summary of clinical, anatomical and biomechanical data of the sixteen cases studied. (U=Unruptured, R=Ruptured, U-PRS = Unruptured with pre-rupture symptoms, MCA =Middle Cerebral Artery, PComA = Posterior Communicating Artery, ICA = Internal Carotid Artery).The tissue classification (Soft/Rigid/Intermediate) is done according to the graphs shown in fig.4 et 5.

Female Subgroup	Location	Cumulative Documented Risk Factors	Aneurysm Status	Thickness (µm)	Biomechanical properties	C <sub>10</sub> (MR3) MPa	C <sub>01</sub> (MR3) MPa	C <sub>11</sub> (MR3) MPa	Statistical Error
Aneurysm 3	MCA	0	<b>R</b>	420	Soft	0	0.0639	0.124	0.001
Aneurysm 4	ACA	2	<b>R</b>	300	Soft	0	0.0516	0.23	0.064
Aneurysm 16	ICA	1	<b>U-PRS</b>	380	Soft	0	0.04497	0.3077	0.00465
Aneurysm 6	PCA	5	<b>R</b>	450	Soft	0.02936	0	1.259	0.0355
Aneurysm 8	MCA	2	U	420	Intermediate	0.019057	0	2.196	0.0345
Aneurysm 11	MCA	5	U	390	Intermediate	0.0431	0	2.428	0.039
Aneurysm 10	ICA	5	U	310	Intermediate	0	0.0352	2.482	0.05
Aneurysm 15	PCA	1	U	680	Intermediate	0	0.06582	4.295	0.0433
Aneurysm 2	MCA	1	U	390	<b>Rigid</b>	0.376	0	<b>18.847</b>	0.033
Aneurysm 9	MCA	5	U	260	<b>Rigid</b>	0.2359	-0	<b>19.56</b>	0.049
Aneurysm 7	MCA	1	U	310	<b>Rigid</b>	0.7705	0	<b>32.149</b>	0.0067

Male Sub-group	Location	Cumulative Documented Risk Factors	Aneurysm Status	Thickness (µm)	Biomechanical properties	C <sub>10</sub> (MR3) MPa	C <sub>01</sub> (MR3) MPa	C <sub>11</sub> (MR3) MPa	Statistical Error
Aneurysm 5	ACA	1	<b>R</b>	330	Soft	0.1803	0	3.241	0.016
Aneurysm 13	ACA	1	<b>R</b>	290	Soft	0.9374	0	3.101	0.0267
Aneurysm 12	MCA	2	U	170	Intermediate	0.1951	0	14.987	0.0457
Aneurysm 14	MCA	1	U	200	Intermediate	0.1015	0	7.9232	0.04
Aneurysm 1	MCA	1	U	620	<b>Rigid</b>	0.2569	0	<b>12.265</b>	0.035

**Table 2:** Comparison of clinical and biomechanical parameters between the three identified tissue subgroups in the overall population.

n = 16	Aneurysmal wall biomechanical classification	n	Mean	p
<b>Risk Factors</b>	INTERMEDIATE	6	2.6	0.456
	SOFT	6	1.6	.
	RIGID	4	2	.
<b>Wall Thickness</b>	INTERMEDIATE	6	360	0.994
	SOFT	6	361	.
	RIGID	4	392	.
<b>C10</b>	INTERMEDIATE	6	0.0598	0.057
	SOFT	6	0.1911	.
	RIGID	4	0.3916	.
<b>C01</b>	INTERM	6	0.0168	0.792
	SOFT	6	0.0267	.
	RIGID	4	0.0322	.
<b>C11</b>	INTERM	6	5.71	<.001**
	SOFT	6	1.37	.
	RIGID	4	20.87	.

**Table 3:** Comparison of clinical data and biomechanical parameters between Ruptured and Unruptured aneurysms in the overall population (male and female).

	Status	n	Mean	p
Risk factors	<b>Ruptured</b>	6	1.66	0.366
	Unruptured	10	2.4	.
Wall Thickness	<b>Ruptured</b>	6	0.36	0.918
	Unruptured	10	0,37	.
C10	<b>Ruptured</b>	6	0.19	0.404
	Unruptured	10	0.19	.
C01	<b>Ruptured</b>	6	0.026	0.757
	Unruptured	10	0.023	.
C11	<b>Ruptured</b>	6	1.377	0.004***
	Unruptured	10	11.78	



**Table 4:** Comparison of clinical data and biomechanical parameters between Ruptured and Unruptured aneurysms in the female group.

	Status	n	Mean	p
Risk factors	<b>Ruptured</b>	4	2	0.516
	Unruptured	7	2.85	.
Wall Thickness	<b>Ruptured</b>	4	388	0.861
	Unruptured	7	392	.
C10	<b>Ruptured</b>	4	0.00734	0.200
	Unruptured	7	0.20637	.
C01	<b>Ruptured</b>	4	0.04012	0.279
	Unruptured	7	0.01443	.
C11	<b>Ruptured</b>	4	0.48	0.001**
	Unruptured	7	11.70	

**Table 5:** Comparison of clinical data and biomechanical parameters between Ruptured and Unruptured aneurysms in the male group.

	Status	n	Mean	p
Risk factors	<b>Ruptured</b>	2	1	0.495
	Unruptured	3	1.3	.
Wall Thickness	<b>Ruptured</b>	2	309	0.638
	Unruptured	3	329	.
C10	<b>Ruptured</b>	2	0.558	0.638
	Unruptured	3	0.160	.
C01	<b>Ruptured</b>	2	-0.0001	0.638
	Unruptured	3	0.043	.
C11	<b>Ruptured</b>	2	3.17	0.058
	Unruptured	3	11.95	.

## REFERENCES:

1. Wardlaw JM, White PM. The detection and management of unruptured intracranial aneurysms. *Brain*. 2000;123 ( Pt 2):205-221
2. Sluzewski M, Bosch JA, van Rooij WJ, Nijssen PC, Wijnalda D. Rupture of intracranial aneurysms during treatment with guglielmi detachable coils: Incidence, outcome, and risk factors. *J Neurosurg*. 2001;94:238-240
3. Unruptured intracranial aneurysms--risk of rupture and risks of surgical intervention. International study of unruptured intracranial aneurysms investigators. *N Engl J Med*. 1998;339:1725-1733
4. Asari S, Ohmoto T. Natural history and risk factors of unruptured cerebral aneurysms. *Clin Neurol Neurosurg*. 1993;95:205-214
5. Wiebers DO, Whisnant JP, Sundt TM, Jr., O'Fallon WM. The significance of unruptured intracranial saccular aneurysms. *J Neurosurg*. 1987;66:23-29
6. Kyriacou SK, Humphrey JD. Influence of size, shape and properties on the mechanics of axisymmetric saccular aneurysms. *J Biomech*. 1996;29:1015-1022
7. Isaksen JG, Bazilevs Y, Kvamsdal T, Zhang Y, Kaspersen JH, Waterloo K, Romner B, Ingebrigtsen T. Determination of wall tension in cerebral artery aneurysms by numerical simulation. *Stroke*. 2008;39:3172-3178
8. Alnaes MS, Isaksen J, Mardal KA, Romner B, Morgan MK, Ingebrigtsen T. Computation of hemodynamics in the circle of willis. *Stroke*. 2007;38:2500-2505
9. Cebal JR, Castro MA, Appanaboyina S, Putman CM, Millan D, Frangi AF. Efficient pipeline for image-based patient-specific analysis of cerebral aneurysm hemodynamics: Technique and sensitivity. *IEEE Trans Med Imaging*. 2005;24:457-467
10. Radaelli AG, Augsburg L, Cebal JR, Ohta M, Rufenacht DA, Balossino R, Benndorf G, Hose DR, Marzo A, Metcalfe R, Mortier P, Mut F, Reymond P, Socci L, Verhegghe B, Frangi AF. Reproducibility of haemodynamical simulations in a subject-specific stented aneurysm model--a report on the virtual intracranial stenting challenge 2007. *J Biomech*. 2008;41:2069-2081
11. Hoi Y, Meng H, Woodward SH, Bendok BR, Hanel RA, Guterman LR, Hopkins LN. Effects of arterial geometry on aneurysm growth: Three-dimensional computational fluid dynamics study. *J Neurosurg*. 2004;101:676-681
12. Cebal JR, Mut F, Weir J, Putman C. Quantitative characterization of the hemodynamic environment in ruptured and unruptured brain aneurysms. *AJNR Am J Neuroradiol*. 2011;32:145-151
13. Cebal JR, Mut F, Weir J, Putman CM. Association of hemodynamic characteristics and cerebral aneurysm rupture. *AJNR Am J Neuroradiol*. 2011;32:264-270
14. Scott S, Ferguson GG, Roach MR. Comparison of the elastic properties of human intracranial arteries and aneurysms. *Can J Physiol Pharmacol*. 1972;50:328-332
15. Toth BK, Nasztanovics F, Bojtár I. Laboratory tests for strength parameters of brain aneurysms. *Acta Bioeng Biomech*. 2007;9:3-7
16. Masson I, Fialaire-Legendre A, Godin C, Boutouyrie P, Bierling P, Zidi M. Mechanical properties of arteries cryopreserved at -80 degrees c and -150 degrees c. *Med Eng Phys*. 2009;31:825-832
17. Karmonik C, Diaz O, Grossman R, Klucznik R. In-vivo quantification of wall motion in cerebral aneurysms from 2d cine phase contrast magnetic resonance images. *Rofo*. 2010;182:140-150
18. Ogden GAHaRW. Biomechanical modelling at the molecular, cellular and tissue levels. *CISM Courses and Lectures, Springer: Wien, New York*. 2009;No. 508: 259-343
19. Marc André Meyers P-YC, Albert Yu-Min Lin, Yasuaki Seki. Biological materials: Structure and mechanical properties, review article. *Progress in Materials Science*. 2008;Volume 53:1-206

20. Oliver A, Shergold NAFaDR. The uniaxial stress versus strain response of pig skin and silicone rubber at low and high strain rates. *International Journal of Impact Engineering*. 2006;Volume 32:1384-1402
21. Mooney M. A theory of large elastic deformation. *Journal of Applied Physics*. 1940;11:582-592.
22. Rivlin RS. Large elastic deformations of isotropic materials. I. *Fundamental concepts, Philosophical Transactions of the Royal Society of London. Series A, Mathematical and Physical Sciences*. 1948; 240:459-490.
23. Low SK, Zembutsu H, Takahashi A, Kamatani N, Cha PC, Hosono N, Kubo M, Matsuda K, Nakamura Y. Impact of limk1, mmp2 and tnfr-alpha variations for intracranial aneurysm in japanese population. *J Hum Genet*. 2011
24. Crawford T. Some observations on the pathogenesis and natural history of intracranial aneurysms. *J Neurol Neurosurg Psychiatry*. 1959;22:259-266
25. Frosen J, Piippo A, Paetau A, Kangasniemi M, Niemela M, Hernesniemi J, Jaaskelainen J. Remodeling of saccular cerebral artery aneurysm wall is associated with rupture: Histological analysis of 24 unruptured and 42 ruptured cases. *Stroke*. 2004;35:2287-2293
26. Watton PN, Ventikos Y, Holzapfel GA. Modelling the growth and stabilization of cerebral aneurysms. *Math Med Biol*. 2009;26:133-164
27. Krings T, Willems P, Barfett J, Ellis M, Hinojosa N, Blobel J, Geibprasert S. Pulsatility of an intracavernous aneurysm demonstrated by dynamic 320-detector row cta at high temporal resolution. *Cen Eur Neurosurg*. 2009;70:214-218
28. Hayakawa M, Katada K, Anno H, Imizu S, Hayashi J, Irie K, Negoro M, Kato Y, Kanno T, Sano H. Ct angiography with electrocardiographically gated reconstruction for visualizing pulsation of intracranial aneurysms: Identification of aneurysmal protuberance presumably associated with wall thinning. *AJNR Am J Neuroradiol*. 2005;26:1366-1369
29. Ishida F, Ogawa H, Simizu T, Kojima T, Taki W. Visualizing the dynamics of cerebral aneurysms with four-dimensional computed tomographic angiography. *Neurosurgery*. 2005;57:460-471; discussion 460-471
30. MacDonald DJ, Finlay HM, Canham PB. Directional wall strength in saccular brain aneurysms from polarized light microscopy. *Ann Biomed Eng*. 2000;28:533-542
31. Zhang C, Villa-Uriol MC, De Craene M, Pozo JM, Frangi AF. Morphodynamic analysis of cerebral aneurysm pulsation from time-resolved rotational angiography. *IEEE Trans Med Imaging*. 2009;28:1105-1116
32. Balocco S, Camara O, Vivas E, Sola T, Guimaraens L, Gratama van Andel HA, Majoie CB, Pozo JM, Bijmens BH, Frangi AF. Feasibility of estimating regional mechanical properties of cerebral aneurysms in vivo. *Med Phys*. 2010;37:1689-1706
33. Zhao X, Raghavan ML, Lu J. Identifying heterogeneous anisotropic properties in cerebral aneurysms: A pointwise approach. *Biomech Model Mechanobiol*. 2011;10:177-189

543  
544  
545 **Conflict of interest statement**  
546 All authors do not have any financial and personal relationships with other people or organi-  
547 sations that could inappropriately influence this work.  
548  
549

549

550 **Acknowledgement:**

551 The authors would like to thank Philips™, Ansys™, for funding part of this research and pro-  
552 viding free research software licenses. These sources of funding were not involved in the  
553 study design, in the collection, analysis and interpretation of data; in the writing of the manu-  
554 script; and in the decision to submit the manuscript for publication.

555